Rock and Soil Mechanics

Volume 44 | Issue 2 Article 3

4-10-2023

Experimental research on the shear characteristics of the composite liner consisting of wrinkled geomembrane and needle punched geosynthetic clay liner

Hai LIN
School of Infrastructure Engineering, Nanchang University, Nanchang, Jiangxi 330031, China, Key Laboratory of Tailings Reservoir Engineering Safety of Jiangxi Province, Nanchang University, Nanchang, Jiangxi 330031, China

Yi-fan ZENG
School of Infrastructure Engineering, Nanchang University, Nanchang, Jiangxi 330031, China

Chuang-bing ZHOU
School of Infrastructure Engineering, Nanchang University, Nanchang, Jiangxi 330031, China, Key Laboratory of Tailings Reservoir Engineering Safety of Jiangxi Province, Nanchang University, Nanchang, Jiangxi 330031, China

Ping-xiao DONG
School of Infrastructure Engineering, Nanchang University, Nanchang, Jiangxi 330031, China

Recommended Citation

LIN, Hai; ZENG, Yi-fan; ZHOU, Chuang-bing; DONG, Ping-xiao; and SHI, Jian-yong (2023) "Experimental research on the shear characteristics of the composite liner consisting of wrinkled geomembrane and needle punched geosynthetic clay liner," *Rock and Soil Mechanics*: Vol. 44: Iss. 2, Article 3.
DOI: 10.16285/j.rsm.2022.5357
Available at: https://rocksoilmech.researchcommons.org/journal/vol44/iss2/3

Experimental research on the shear characteristics of the composite liner consisting of wrinkled geomembrane and needle punched geosynthetic clay liner

Authors

Hai LIN, Yi-fan ZENG, Chuang-bing ZHOU, Ping-xiao DONG, and Jian-yong SHI

Rock and Soil Mechanics 2023 44(2): 355−361 ISSN 1000−7598
https: //doi.org/10.16285/j.rsm.2022.5357 http://rocksoilmech.researchcommons.org/journal

Experimental research on the shear characteristics of the composite liner consisting of wrinkled geomembrane and needle punched geosynthetic clay liner

LIN Hai[1, 2], ZENG Yi-fan[1], ZHOU Chuang-bing[1, 2], DONG Ping-xiao[1], SHI Jian-yong[3]

1. School of Infrastructure Engineering, Nanchang University, Nanchang, Jiangxi 330031, China
2. Key Laboratory of Tailings Reservoir Engineering Safety of Jiangxi Province, Nanchang University, Nanchang, Jiangxi 330031, China
3. Geotechnical Research Institute, Hohai University, Nanjing, Jiangsu 210098, China

Abstract: Wrinkles in geomembrane are common among anti-seepage engineering. However, the wrinkling effect has been neglected in most of the current studies on the interface shear properties of geomembrane. The composite liner consisting of a textured geomembrane (GM) and a needle punched geosynthetic clay liner (GCL) was taken as the research object, and the hydration deformation tests confirmed that the two-step hydration method was effective in accelerating the hydration of the wrinkled GM+GCL composite liner. The shear properties of the wrinkled GM+GCL composite liner was studied by a large-scale temperature-controlled submerged direct shear apparatus. The shear characteristic of the wrinkled GM+GCL composite liner was analyzed compared to the shear results of the composite liner without GM wrinkle, and the influence mechanism of GM wrinkles on the shear characteristics of the composite liner was clarified. Experimental results show that the existence of GM wrinkle will change the shear stress–displacement curve of the GM+GCL composite liner a lot, and the peak shear strength of the composite liner under low normal stress can be obviously reduced by the GM wrinkle. Significant progressive failure could be observed in the wrinkled GM+GCL composite liner. Additionally, multiple failure modes can coexist inside the composite liner under unique normal stress as well.
Keywords: geomembrane; wrinkle; geosynthetic clay liner; shear strength; failure modes

1 Introduction

Geomembranes are commonly used as impermeable structures in landfills, reservoir dams and mine tailings repositories, but factors such as temperature rise or nonuniform deformation make geomembrane wrinkled widespread[1–11]. For example, during the construction and laying period of the geomembrane or the gap period of uncompleted soil filling after the geomembrane laying for landfill lining structure, the geomembrane surface temperature changes periodically due to solar irradiation, climate change and ambient temperature difference between day and night, which in turn causes the geomembrane to expand and deform, forming significant wrinkles (see Fig.1). Rowe et al.[12] conducted field observations and analysis of geomembranes laid on slopes and confirmed that solar illumination and air temperature were the main factors affecting the generation of wrinkles of exposed geomembranes, and field tests showed that the maximum height of geomembrane wrinkles could reach 180 mm and the width of wrinkles could reach 200–300 mm. The thickness and type of geomembrane, the area of the restricted deformation zone and the type of subsoil all have an influence on the length, height and width of the geomembrane wrinkles[12–13]. Laboratory tests also reproduce the geomembrane wrinkle phenomenon, and the shape of the wrinkle can be well characterized by a Gaussian distribution[9]. After the formation of geomembrane wrinkles, the wrinkles persist even though a decrease in geomembrane surface temperature results in a significant reduction in wrinkle height[9]. When geomembranes containing wrinkles are covered with soil and pressurized up to 1 100 kPa, the void between the geomembrane wrinkle and the underlying compacted clay does not disappear[12, 14]. Geomembranes in hydraulic and slope works are subjected to temperature or sunlight for short period or long period, and geomembranes in impermeable structures such as landfills or tailings/ metallurgical waste repositories may be subjected to high temperatures resulting from waste degradation or chemical reactions. Therefore the creased state of geomembranes is a necessary feature of engineering applications.

Fig. 1 Picture of wrinkled GM

The composite liner consisting of textured geomembrane (GM) and a needle-punched geosynthetic clay liner (GCL) is widely used in the bottom liner of landfills due to its good hydraulic impermeability properties, and the shear strength of the GM+GCL composite

Received: 24 March 2022 Accepted: 30 May 2022
This work was supported by the National Natural Science Foundation of China (42062018, 41702324, U1765207, 41530637).
First author: LIN Hai, male, born in 1986, PhD, Associate Professor, mainly engaged in teaching and research in geotechnical and foundation engineering, environmental geotechnical engineering. E-mail: linhai@ncu.edu.cn

interface is a key factor in the safety analysis of landfill liner slope stability. The GM/GCL interface and the internal interface of GCL exhibit a low interfacial shear strength after hydration, and single interface shear tests were once the primary means of determining the shear strength properties of composite liners containing GCL[15–16]. Recent experimental studies have shown that shear testing of GM+GCL composite liners without a confined shear failure surface provides a more intuitive reflection of the true shear properties of composite liners than single interface shear testing[17]. Most of the shear test studies on GCL liners have been conducted at room temperature and under GM wrinkle-free conditions, and the temperature effect on the shear strength of composite interfaces containing GCL has been a research hotspot in current worldwide[18–20]. Some scholars have established a quantitative connection between GM wrinkle and the permeability properties of composite liners[21]. However, no studies on the shear properties of geosynthetic interfaces in the case of geomembrane wrinkles have been reported up to now, and the shear properties of composite liners containing wrinkled GM+GCL are still unknown.

To investigate and analyze the overall shear properties of the composite liner when the geomembrane is wrinkled and thus to objectively consider the influence of geomembrane wrinkles in geomembrane slope stability analysis, a large-scale temperature- controlled saturated direct shear instrument was used to conduct an overall shear test on the GM+GCL composite liner. By comparing the shear strength pattern and damage morphology of the composite liner with and without wrinkles in GM, the quantitative influence of geomembrane wrinkles on the shear properties of the composite liner is revealed. The research results will hopefully provide an experimental basis and theoretical support for improving the slip stability analysis of geomembranes and other geosynthetic reinforced slopes.

2 Materials and method

2.1 Test materials and equipment

The geosynthetic material used in this test is a 2 mm thick single textured HDPE geomembrane (GM) provided by Changsha Jianyi New Materials Co., Ltd., and a needle-punched geosynthetic clay liner (GCL) provided by Shanghai Renzhong Industrial Co., Ltd., where the GCL is formed by sandwiching between natural sodium bentonite between a layer of woven fabric and a layer of non-woven fabric and being reinforced using needling. The physical and mechanical parameters of the geosynthetic material are shown in Table 1.

Table 1 Mechanical parameters of geosynthetics

Textured geomembrane					Needle-punched geosynthetic clay liner				
Texture height /mm	Density /(g • m^{-3})	Elongation at yield /%	Yield strength /(N • mm^{-1})	Puncture strength /N	Mass-to-area ratio /(g • m^{-2})	Tensile strength /(N • cm^{-1})	Peel strength /(N • cm^{-1})	Expansion coefficient /(mL • g^{-1})	Normal hydraulic conductivity /(cm • s^{-1})
0.25	0.94	12	29	534	5 000	156	11.4	12.5	4.32×10^{-9}

The shear test on the GM+GCL composite liner with wrinkle was carried out using a large-scale temperature-controlled submerged direct shear apparatus from the Geotechnical Laboratory of Nanchang University, as shown in Fig.2, and a schematic diagram of the apparatus operation can be found in the literature[20]. The apparatus can achieve a specimen shear area of 300 mm×300 mm and can keep the specimen submerged in a constant temperature throughout the shearing process. The applied maximum normal and shear stresses are all 2.2 MPa, the maximum shear displacement is 45 mm, the shear rate ranges from 0.01 to 10 mm/min, and the temperature range is 0–70 ℃.

Because of the stiffness of the HDPE geomembrane, the artificially produced wrinkles make it more difficult to fix the GM on the back side in shear tests than to fix the GM without wrinkles. To solve the problem of fixing the GM at the interface, a special stainless steel grooved plate was fabricated (see Fig.3). Both sides of the groove are densely covered with adjustable teeth with a height of 0–1 mm, which increase the friction between the geomembrane and the grooved plate and fix the geomembrane to the surface of the grooved plate. The distribution of GM wrinkles in actual engineering is random, and the spacing between adjacent GM wrinkles obtained in geomembrane field

Fig. 2 Diagram of large-scale temperature-controlled submerged direct shear apparatus

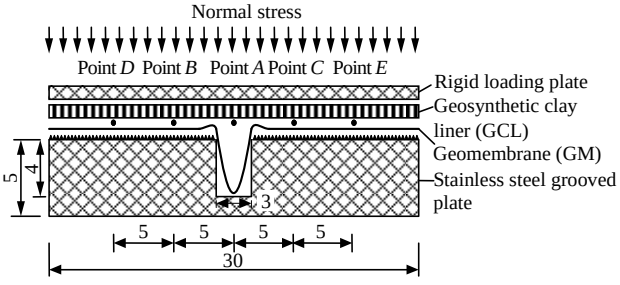

Fig. 3 Schematic diagram of hydration deformation test of wrinkled GM+GCL composite liner (unit: cm)

tests[12–13] carried out by Queen's University in Canada was mostly close to 3 m, while the width of GM wrinkles was mostly about 0.3 m. Therefore, this experimental study drew on this approximate width ratio of GM wrinkles in the previous experiment and set the width of the groove as 30 mm and the height as 40 mm for a 300 mm side length of the shear plane.

2.2 Hydration steps for wrinkled GM+GCL composite liners

The complete hydration of GCL-containing composite liners under normal pressure usually takes a considerable amount of time, which can seriously affect the efficiency of conducting shear tests on GCL-containing composite liners. Fox et al.[22–24] proposed a two-step hydration method to accelerate the shearing of GCL-containing composite liner geomembranes without wrinkles based on a large number of experimental studies. However, the presence of geomembrane wrinkles in this test resulted in uneven swelling and deformation of the needle-punched geosynthetic clay liner during the hydration, thus the applicability of the traditional two-step hydration method in this test is questionable. For this reason, hydration deformation tests were conducted on wrinkled GM+GCL composite liner under direct and stepwise hydration conditions, and the hydration deformation test setup is schematically shown in Fig. 3. Rectangular specimens of 300 mm×300 mm and 300 mm×370 mm were cut from the same roll of GCL and GM materials, respectively, being careful to avoid damage to the surface of the geosynthetic specimens and loss of bentonite clay trapped within the GCL. The GM specimen was bent into the grooved plate along the middle and made into a wrinkle as shown in Fig.3, and the back of the geomembrane was bonded with epoxy resin glue to the surface of the sharp teeth of the grooved plate. The GCL was laid directly on the GM, and the change in thickness of the GCL at points *A*, *B*, *C*, *D* and *E* were measured continuously as the hydration time increased.

The direct and stepwise hydration methods for the hydration deformation test of the wrinkled GM+GCL composite liners are based on the hydration procedure for GCL in the condition of GM without wrinkles. The direct hydration step is as follows. Lay the specimens in a transparent water tank according to Fig.3, apply a uniform normal pressure of 10 kPa and then add water until the water surface is 3 cm above the rigid sheet. The stepwise hydration step is: firstly exert a small load of 0.1 kN first, adde water until the rigid sheet is submerged 3 cm and stand for hydration for 2 days, and then added a normal pressure of 10 kPa on the specimen. A transparent scale is attached to the outer surface of the transparent water tank at locations *A*, *B*, *C*, *D* and *E* to observe the change in GCL thickness at each point, with the frequency of observation being twice within 1 h of completion of the water addition, and then once every 1 d.

The thickness of dry GCL was about 0.6 cm. The variation of GCL thickness in the wrinkled GM+GCL composite liners after different hydration steps over time is plotted in Fig.4. The results of the observations indicated that the data of the direct hydration method tended to be stable after 16 d, with the GCL thicknesses at each point remaining stable with 0.92, 0.77, 0.53, 0.94 and 0.53 cm at points *A*, *B*, *C*, *D* and *E*. In contrast, the stepwise hydration method remained stable after 2 d, with the GCL thicknesses at each point remaining stable with 0.68, 0.67, 0.37, 0.58, and 0.48 cm at points *A*, *B*, *C*, *D* and *E*. The results of the above two hydration methods resulted in a change of approximately 50% compared to the initial thickness. The results of the hydration deformation tests with the wrinkled GM+GCL composite liner confirmed that the two-step hydration method was able to reduce the hydration time from more than 15 d to less than 2 d. Therefore, the two-step hydration method is also applicable to the shear tests in this paper.

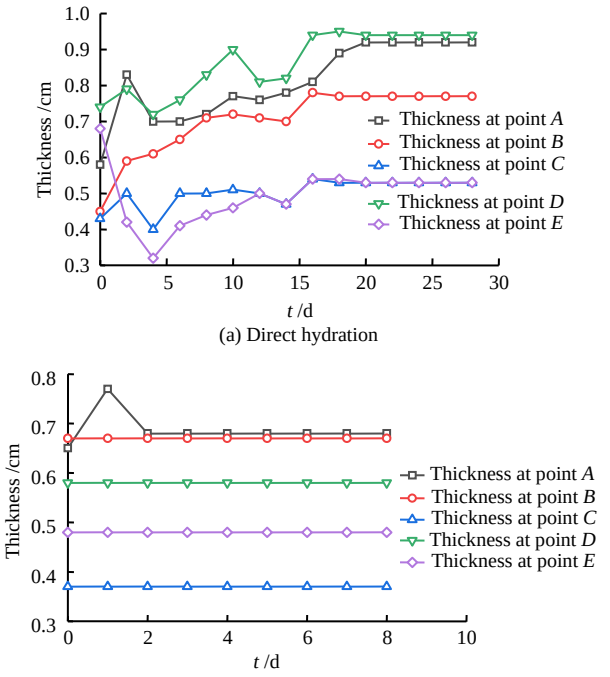

Fig. 4 Time-dependent relationship of GCL thickness in the wrinkled GM+GCL composite liners

2.3 Shear test method and procedure

Firstly, cut out square GCL specimens with a size of 300 mm×300 mm and rectangular GM specimens with a size of 300 mm×470 mm and place GCL specimens in water tank for 2 d. Adjust the sharp teeth on the surface of the grooved steel plate to a suitable height according to the test pressure[25], place the entire lower shear box into the saturated water tank, and then place the rigid pads, grooved steel plate and GM specimens into the lower shear box in turn. To solve the problem of area correction and fixation of the GM specimen during shearing, the length of the cut GM specimen was longer than that of the GCL specimen and the excess part was extended over the surface of the lower shear box to simulate wrinkles. GM wrinkles were produced in the same manner as the lay-up pattern in Fig.3, with the back of the GM

held in place by a combination of pointed teeth and epoxy glue. Once the GM specimen with wrinkles was in place, the initially hydrated needle-punched GCL specimen was placed in the upper shear box and fitted directly to the GM in the lower shear box. After completion of the upper shear box installation, the water tank for submerging specimens was filled with water until the water level was more than 2 cm above the top surface of the shear specimen. Finally, the tank cover was installed, the submerged entire direct shear apparatus was pushed into the loading frame, and the displacement transducer was installed. The normal stresses for this shear test were 100, 200, 300, 500, 700, 900, 1 300 and 1 800 kPa, covering most of the possible stresses for the bottom lining of the landfill. After the application of normal stress, the specimens were allowed to continue to hydrate and consolidate for 1 d before shear was initiated. The lower shear rate is more reflective of the hazardous slip scenario of GCL, and then this paper set the shear rate as 0.1 mm/min based on previous studies[22–24]. Furthermore, to exclude the influence of room temperature variation on the test results, the hydration, pressurization, solidification and shearing of the submerged GCL were carried out at a uniform temperature of 30 ℃.

3 Stress–displacement relationship

The shear stress–displacement relationships for the GM+GCL composite liner for the two cases of GM without wrinkles and GM with wrinkles at a normal pressure of 200 kPa and 1 300 kPa, respectively are shown in Fig.5. The presence of wrinkles resulted in a more obvious difference in the shear stress–displacement relationship for the composite liner, with a variation in shear strength of up to 44%. Figure 5 shows that the strain softening of the composite liner under shear still exists even in the wrinkled GM conditions, and a small peak stress inflection point can still be observed in the shear stress–displacement curve of the wrinkled GM+GCL composite liner. The displacements required to reach the peak shear strength and the small peak stress inflection point for the GM+GCL composite liner with wrinkles were similar to those for the GM without wrinkles, with a difference of only 1 to 2 mm. At 200 kPa, the stress–displacement curve for the GM+GCL composite liner with wrinkles was significantly lower than that for the GM+GCL composite liner without wrinkles in the same condition. However, at 1 300 kPa, the shear stress–displacement curve for the GM+GCL composite liner with wrinkles was higher than that for the GM without wrinkles. It indicated that the presence of GM wrinkles had a significant effect on the shear strength of the composite liner, and this effect did not simply enhance or weaken the interfacial shear strength.

The initial analysis reveals that the contact area of the GM/GCL interface and the height of the GCL bulge in the wrinkle area contribute to this difference in strength. Under a low normal stress, the contact area plays a major role, and the appearance of GM wrinkles reduced the contact area of the GM/GCL interface, which leads to a reduction in the shear strength of the GM+GCL composite liner. Under a higher normal stress, the normal stress and shear stress drive the hydrated bentonite to migrate towards the direction of the wrinkles and give rise to a local bulge on the GCL surface. Consequently, the local bulge resists the shear of the GCL composite liner, thereby increasing the peak shear strength of the GM+GCL composite liner.

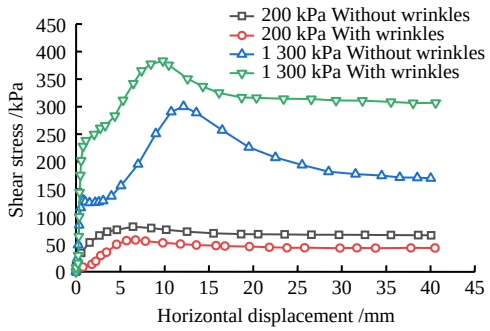

Fig. 5 Influence of wrinkled GM on shear stress-displacement relationship of composite liners

The stress–displacement relationship for the wrinkled GM+GCL composite liners under different normal pressures is presented in Fig. 6.

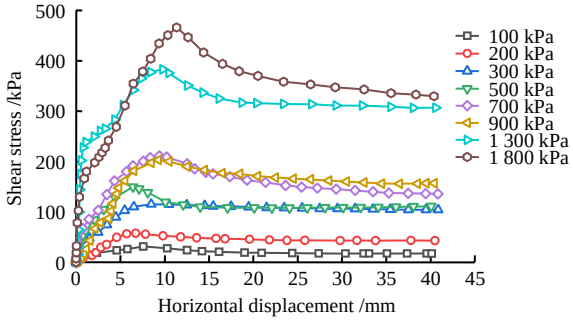

Fig. 6 Shear stress–displacement curves of wrinkled GM+GCL composite liners under different normal stresses

Figure 6 shows that the shear stress of the composite liner reaches a peak and then gradually decrease and reaches a more stable large displacement shear strength for all levels of stress conditions within the shear displacement range of this test. The peak shear strength of the wrinkled GM+GCL composite liner and its corresponding peak shear displacement both increase with the increase of normal stress, however, the shear stress–displacement curves of the wrinkled GM+GCL composite liner are not as uniform as that without wrinkles. As shown in Fig.6, the small peak stress inflections in the stress–displacement curve of the composite liner at some pressures (e.g., 700 kPa) are no longer evident, in contrast to the obvious small peak inflection in the without wrinkles under the same conditions[15, 25].

The shear displacement required to reach peak strength for the wrinkled GM+GCL composite liner

(peak shear displacement) is illustrated in Fig. 7. Overall, the shear peak displacement of the GM+GCL composite liner increases with increasing normal stress in both cases of geomembrane without wrinkles or with wrinkles. The peak shear displacement of the GM+GCL composite liner with wrinkles is on average 1.3 mm smaller than that without wrinkles, a reduction of 7.4%. GM wrinkles make the composite liners require smaller shear displacements to achieve peak shear strength.

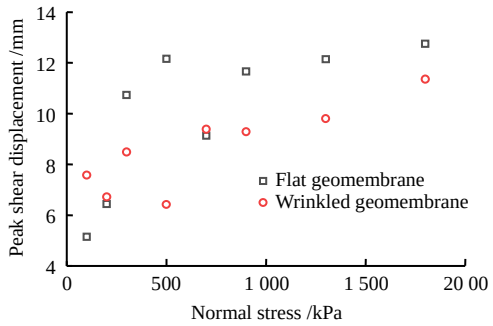

Fig. 7 Influence of wrinkled GM on the peak shear displacement of composite liners

4 Destruction mode

In this test, the damage state of the wrinkled GM+GCL composite liner after shear completion was carefully observed and analyzed. According to the naked eye observation of the GCL surface and the cut inside, it was found that the normal pressure had a significant effect on the damage mode of the hydrated needle-punched GCL. The GCL specimens after the composite liner shear completion are shown in Fig. 8, and the GCL specimens were divided into two parts, the front and the back parts, with the shear direction as the reference direction. When 100 kPa$\leqslant\sigma_{\mathrm{n}}\leqslant$300 kPa, there was only a weak bulge on the surface of the GCL specimen, in this case, the shear displacement occurred only at the GM/GCL interface, as shown in Fig. 8(a). When 500 kPa$\leqslant\sigma_{\mathrm{n}}\leqslant$700 kPa, the surface of the GCL specimen already had an obvious bulge at the contact position with the GM wrinkles, and the front part of the specimen did not slip significantly during the shear process, while the back part of the specimen showed an obvious slip, as shown in Fig. 8(b). The needle-punched fibers on the front part of the specimen were slightly stretched and elongated when the GCL specimen was cut along the middle bentonite layer. This indicated that the front part of the GCL specimen was sheared at the GM/GCL interface only, while the back part was sheared at the GM/GCL interface and inside the GCL at the same time. The surface of the GCL specimen at the contact position with the GM wrinkles was raised to a height of about 8.5 mm when 900 kPa$\leqslant\sigma_{\mathrm{n}}\leqslant$1 300 kPa, and the surface of the front part of the GCL specimen was locally distorted; the internal fibers of the GCL specimen on the back part were completely pulled off, and the morphology of the GCL specimen at this point after gently lifting the geotextile on one side is shown in Fig.8(c). It is inferred that both GM/GCL interfacial shear damage and internal interfacial damage occur on the front part of the GCL specimen, while internal shear damage of GCL is predominant on the rear part of the GCL specimen. At a high normal pressure of $\sigma_{\mathrm{n}}=1\,800$ kPa, the surface bulge of the GCL specimen could reach a maximum height of about 13 mm. It is clearly seen that the two layers of geotextile in the GCL specimen were staggered, which means that the fibers on both sides were completely pulled off, and the shear damage on both parts of the GCL was from the internal interface, as shown in Fig. 8(d). In summary, GM wrinkles had a significant effect on the damage pattern of the GCL in the composite liner, with the height of the GCL surface bulge increasing with increasing normal pressure. A clear progressive damage pattern occurred in the front and back parts of the GCL, bounded by the wrinkle position, with the back part of the GCL specimen being the first to shift from interfacial damage to internal shear damage with increasing normal pressure σ_{n}.

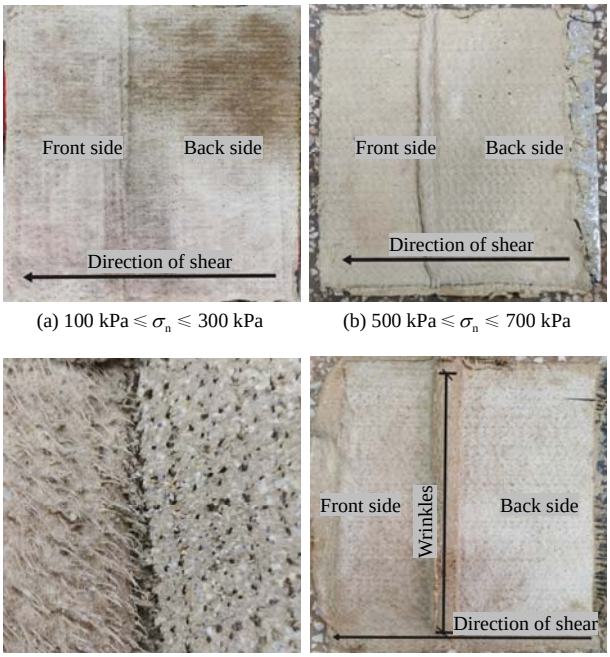

(a) 100 kPa$\leqslant\sigma_{\mathrm{n}}\leqslant$300 kPa (b) 500 kPa$\leqslant\sigma_{\mathrm{n}}\leqslant$700 kPa

(c) 900 kPa$\leqslant\sigma_{\mathrm{n}}\leqslant$1 300 kPa (d) $\sigma_{\mathrm{n}}=1\,800$ kPa

Fig. 8 Failure modes of GCLs under various test conditions

5 Shear strength

The peak strength envelope for the wrinkled GM+GCL composite liner is shown in Fig.9, where the strength envelope displays significant non-linearity, with the shear peak friction angle decreasing with increasing normal stress σ_{n}. The peak strength of the wrinkled GM+GCL composite liner can be better fitted with the Duncan-Chang model, as similar to that without GM wrinkles. The specific formula is as follows.

$$\tau_{\mathrm{p}}=\sigma_{\mathrm{n}}\tan\left[\varphi_0+\Delta\varphi\lg\left(\frac{\sigma_{\mathrm{n}}}{P_{\mathrm{a}}}\right)\right] \quad (1)$$

where τ_p is the peak strength of the composite liner; φ_0 and $\Delta\varphi$ are the model constants obtained by fitting the test results; and P_a is the atmospheric pressure.

The peak strength expressions of the composite liner for the GM with and without wrinkles are shown in Fig. 9. The peak strength envelope of the GM+GCL composite liner with wrinkles was slightly lower than that of the GM without wrinkles at a normal pressure $\sigma_n \leqslant 500$ kPa. The peak friction angle of the GM+GCL composite liner with wrinkles decreases significantly less with increasing normal pressure than that of the GM without wrinkles. At $\sigma_n \geqslant 700$ kPa, the peak strength of GM+GCL composite liner with wrinkles is higher than that without wrinkles. In this test, the difference between the peak shear strength of the wrinkled GM+GCLcomposite liner at $\sigma_n = 1\,800$ kPa and that of the composite liner without wrinkles can be up to 21%.

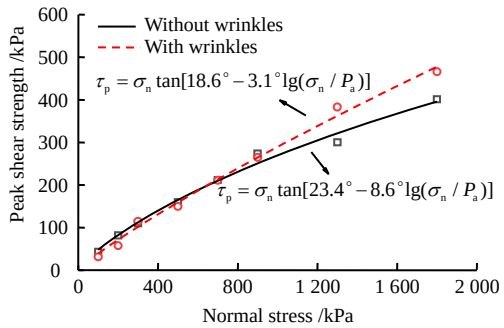

Fig. 9 Influence of wrinkled GM on the peak shear strength of composite liners

The large displacement shear strength (shear displacement $\delta = 40$ mm) envelope for the wrinkled GM+GCL composite liner is shown in Fig.10. Equation (1) also provides a good fit to the large displacement shear strength envelope for the wrinkled GM+GCL composite liner. Like the peak strength envelope, the GM wrinkles reduce the large displacement shear strength of the composite liner at lower normal pressures ($\sigma_n \leqslant 500$ kPa), and the reduction in large displacement shear strength of the composite liner can be up to 52%. Similarly, the tangential friction angle of the large displacement strength of the composite liner with GM wrinkles decreases significantly less with increasing normal pressure than that without GM wrinkles. At $\sigma_n \geqslant 700$ kPa,

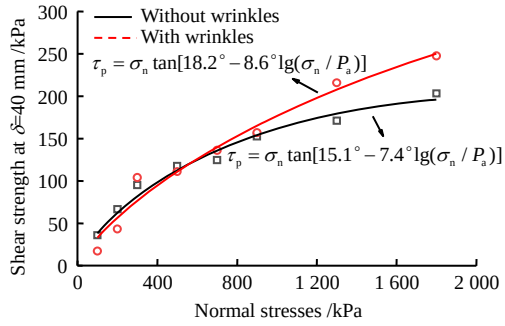

Fig. 10 Influence of wrinkled GM on the large-displacement shear strength of composite liners

the large displacement shear strength of the GM+GCL composite liner with wrinkles become higher than that of the without GM wrinkles, and the difference in large displacement strength of the composite liner due to GM wrinkles alone could be up to 22%.

6 Conclusion

Geomembrane wrinkles are widespread in projects such as landfills and slopes. To investigate the mechanism of geomembrane (GM) wrinkles on the shear strength properties of GM+GCL composite liners, shear tests on GM+GCL composite liners with wrinkles were carried out using a large temperature-controlled submerged direct shear apparatus, and the test results were compared with the shear properties of the composite liners without wrinkles. The main conclusions were drawn as follows.

(1) GM wrinkles caused a significant difference in the shear stress–displacement curve of the composite liner. The shear strength of the composite liner with the GM wrinkles at a low normal pressures was less, while at high normal pressures, GM wrinkles increase the shear strength of the composite liner. The reduction of the GM/GCL contact area at the GM wrinkle position and the expansion and deformation of the GCL at the wrinkle position are the main reasons for this change.

(2) The stress–displacement curve of the wrinkled GM+GCL composite liner still has a distinct peak shear strength and post-peak softening characteristics; the small displacement of stress inflection can be observed in the stress–displacement curve of the composite liner with wrinkles, but it is not as obvious as when the GM is without wrinkles. The peak shear displacement of the wrinkled GM+GCL composite liner increases as the normal pressure increases, but the peak shear displacement of the composite liner is slightly lower than that without wrinkles.

(3) The GM wrinkles has a significant effect on the damage pattern of the composite liner. The height of the GCL surface bulge increases with increasing normal pressure at the GM wrinkle area, with significant progressive damage occurring on both sides of the GCL surface bulge. The GCL specimens in the back part are the first to shift from interfacial damage to internal shear damage with the increase of σ_n.

(4) The shear strength of the GM+GCL composite liner with wrinkles shows a significant non-linear relationship with increasing normal pressure. At a normal pressure $\sigma_n \leqslant 500$ kPa, the peak strength envelope and the large displacement shear strength envelope of the GM+GCL composite liner with wrinkles are both lower than that without GM wrinkles. The effect of GM wrinkles on the shear strength of the composite liner is detrimental to slope stability, and the generation of GM wrinkles should be avoided as far as possible in practical engineering.

References

[1] CHEN Yun-min, SHI Jian-yong, ZHU Wei, et al. A

review of geoenvironmental engineering[J]. China Civil Engineering Journal, 2012, 45(4): 165–182.

[2] XIE Hai-jian, ZHAN Liang-tong, CHEN Yun-min, et al. Comparison of the performance of four types of liner systems in China[J]. China Civil Engineering Journal, 2011, 44(7): 133–141.

[3] SHU Yi-ming, WU Hai-min, JIANG Xiao-zhen. The development of anti-seepage technology with geomembrane on reservoirs and dams in China[J]. Chinese Journal of Geotechnical Engineering, 2016, 38(Suppl.1): 1–9.

[4] BAO Cheng-gang. Study on interface behavior of geosynthetics and soil[J]. Chinese Journal of Rock Mechanics and Engineering, 2006, 25(9): 1735–1744.

[5] WANG Dian-wu, CAO Guang-zhu, WU Yan-qing. Research on the durability law of geosynthetics[J]. Chinese Journal of Geotechnical Engineering, 2005, 27(4): 398–402.

[6] XU Si-fa, YANG Yang, HONG Bo. Evaluation of temperature stress relaxation properties of HDPE sheet[J]. Journal of Southeast University (Natural Science Edition), 2006, 36(5): 820–824.

[7] XU Si-fa, WANG Guo-cai, WANG Zhe. Evaluation of tensile forces of geomembrane placed on waste landfill slope due to temperature variation and filling height[J]. Rock and Soil Mechanics, 2010, 31(10): 3120–3124.

[8] ROWE R K, BRACHMAN R W I, TAKE W A, et al. Field and laboratory observations of down-slope bentonite migration in exposed composite liners[J]. Geotextiles and Geomembranes, 2016, 44: 686–706.

[9] TAKE W A, WATSON E, BRACHMAN R W I, et al. Thermal expansion and contraction of geomembrane liners subjected to solar exposure and backfilling[J]. Journal of Geotechnical and Geoenvironmental Engineering, 2012, 138(11): 1387–1397.

[10] ABUEL-NAGA H M, BOUAZZA A. Thermomechanical behavior of saturated geosynthetic clay liners[J]. Journal of Geotechnical and Geoenvironmental Engineering, 2013, 139(4): 539–547.

[11] TOUZE-FOLTZ N, BANNOUR H, BARRAL C, et al. A review of the performance of geosynthetics for environmental protection[J]. Geotextiles and Geomembranes, 2016, 44: 656–672.

[12] ROWE R K, CHAPPEL M J, BRACHMAN R W I, et al. Field study of wrinkles in a geomembrane at a composite liner test site[J]. Canadian Geotechnical Journal, 2012, 49(10): 1196–1211.

[13] CHAPPEL M J, ROWE R K, BRACHMAN R W I, et al. A comparison of geomembrane wrinkles for nine field cases[J]. Geosynthetics International, 2012, 19(6): 453–469.

[14] BRACHMAN R W I, GUDINA S. Geomembrane strains from coarse gravel and wrinkles in a GM/GCL composite liner[J]. Geotextiles and Geomembranes, 2008, 26: 488–497.

[15] LIN Hai, SHI Jian-yong, QIAN Xue-de. Experimental research on shear failure mechanism of hydrated needle-punched GCLs[J]. Chinese Journal of Geotechnical Engineering, 2017, 39(8): 1374–1380.

[16] LIN Hai, ZHANG Ling-ling. Effect of hydration state on shear strength of composite liner with needle-punched GCL[J]. Chinese Journal of Geotechnical Engineering, 2017, 39(Suppl.1): 219–223.

[17] LIN Hai, ZHANG Ling-ling, RUAN Xiao-bo, et al. Simple-shear failure characteristics of hydrated needle-punched GCL+GM composite liner[J]. Chinese Journal of Geotechnical Engineering, 2016, 38(9): 1660–1667.

[18] HOOR A, ROWE R K. Application of tire chips to reduce the temperature of secondary g eomembranes in municipal solid waste landfills[J]. Waste Management, 2012, 32: 901–911.

[19] SINGH R M, BOUAZZA A. Thermal conductivity of geosynthetics[J]. Geotextiles and Geomembranes, 2013, 39: 1–8.

[20] HAN Zhuo-wei, LIN Hai, SHI Jian-yong. Shear characteristics of hydrated needle-punched GCL+GM composite liners at different temperatures[J]. Chinese Journal of Geotechnical Engineering, 2021, 43(5): 962–967.

[21] CHEN Cheng, ZHAN Liang-tong, XU Wen-jie, et al. Hydraulic connectivity analysis of wrinkle network for geomembrane as composite liner[J]. Rock and Soil Mechanics, 2018, 39(10): 3685–3694.

[22] FOX P J, STARK T D. State-of-the-art report: GCL shear strength and its measurement ten-year update[J]. Geosynthetics International, 2015, 22(1): 3–47.

[23] FOX P J, ROSS J D. Relationship between NP GCL internal and HDPE GMX/NP GCL interface shear strengths[J]. Journal of Geotechnical and Geoenvironmental Engineering, 2011, 137(8): 743–753.

[24] TRIPLETTE E J, FOX P J. Shear strength of HDPE geomembrane/geosynthetic clay liner interfaces[J]. Journal of Geotechnical and Geoenvironmental Engineering, 2001, 127(6): 543–552.

[25] LIN Hai, HAN Zhuo-wei, SHI Jian-yong. Interface shear failure mechanisms and peak strength analysis of geos[J]. Journal of Huazhong University of Science and Technology (Natural Science Edition), 2020, 48(7): 99–106.